

Cation distribution and intrinsic magnetic properties of Co-Ti-doped *M*-type barium ferrite

X. Batlle

Departament Física Fonamental, Universitat de Barcelona, Diagonal 647, 08028 Barcelona, Spain

X. Obradors

Institut de Ciència de Materials de Barcelona, C.S.I.C., Martí i Franquès s/n, 08028 Barcelona, Spain

J. Rodríguez-Carvajal

Institut Laue-Langevin, 156X, 38042 Grenoble Cedex, France

M. Pernet

Laboratoire de Cristallographie, C.N.R.S., 166X, 38042 Grenoble Cedex, France

M. V. Cabafias and M. Vallet

Laboratorio de Magnetismo Aplicado, R.E.N.F.E.-U.C. Madrid, Las Matas, 28290 Madrid, Spain

(Received 13 December 1990; accepted for publication 29 March 1991)

The structural and magnetic properties of $\text{BaFe}_{12-2x}\text{Co}_x\text{Ti}_x\text{O}_{19}$ ($0 \leq x \leq 1.0$) *M*-type barium ferrite have been investigated by means of neutron powder diffraction and high-field magnetization measurements. The cationic distribution and magnetic moments of the five different metallic sublattices are determined and compared to the experimental saturation magnetization. It is found that about 50% of Co ions occupy tetrahedral sites, thus being ineffective in the reduction of the uniaxial magnetic anisotropy, while Ti ions prefer the $4f_{\text{VI}}$ octahedral sites. All in all, a clear hierarchy of sublattice preferences is defined. Although the collinearity of the magnetic structure is progressively broken, mainly above $x \approx 0.7$, the overall behavior remains ferrimagnetic. The strong local spin canting is tentatively attributed to the localization of diamagnetic Ti ions in the $4f_{\text{VI}}$ octahedral sites.

I. INTRODUCTION

Hexagonal ferrites are a large family of hexagonal or rhombohedral ferrimagnetic oxides with interesting applications as permanent magnets, microwave device materials, and magnetic and magneto-optic recording media¹ so that many efforts have been devoted to improve their magnetic characteristics by substitution of Fe^{3+} cations with other diamagnetic or paramagnetic cations.² Their crystal structure can be described by the superposition of some fundamental structural blocks formed by a close packing of hexagonal or cubic stacked layers with $\text{Ba}(\text{Sr,Pb})\text{O}_3$ and O_4 composition. In this framework, the metallic cations are located in octahedral, tetrahedral, and fivefold coordination interstices.^{2,3}

The most largely studied of all these compounds is the *M*-type barium ferrite $\text{BaFe}_{12}\text{O}_{19}$ (*Ba-M*).²⁻⁴ The *M* structure (*SG* $P6_3/mmc$) is symbolically described RSR^*S^* where *R* is a three-layer block (two O_4 containing one BaO_3) with composition $(\text{Ba}^{2+}\text{Fe}_6^{3+}\text{O}_{11})^{2-}$ and *S* is a two O_4 -layer block with composition $(\text{Fe}^{3+}_6\text{O}_8)^{2+}$, where the asterisk means that the corresponding block has been turned 180° around the hexagonal *c* axis. In this structure the metallic cations are distributed within three different kinds of octahedral sites ($2a$, $4f_{\text{VI}}$ and $12k$ sublattices), one tetrahedral site ($4f_{\text{IV}}$ sublattice), and one pseudotetrahedral site [$4e(\frac{1}{2})$ sublattice]. In Table I we summarize the crystallographic characteristics of these five metallic sublattices.

Pure *M*-type barium ferrite $\text{BaFe}_{12}\text{O}_{19}$ is ferrimagnetic below $T_c \approx 720$ K.^{5,6} The magnetic structure model was

suggested for the first time by Gorter⁵ from the application of the Kramers-Anderson indirect exchange theory.⁷ All the magnetic moments are ordered along the hexagonal *c* axis according to the scheme given in Table I. Dominant interactions are those where the superexchange angle ϑ ($\text{Fe}^{3+}-\text{O}^{2-}-\text{Fe}^{3+}$) is near 180° and they become negligible when this angle tends to 90° .⁸ Isalgue *et al.*⁸ reported that, in the scope of the mean-field approximation, the stability of the Gorter-type structure is well established, except for the $12k$ octahedral site, where the strongly competing interactions give rise to the lowest stability of the spin arrangement among all the metallic sublattices. Similar arguments had previously been used by Albanese, Carbuicchio, and Deriu⁹ to interpret Mössbauer spectra of some Al- and Ga-doped *M*-type strontium ferrites. All in all, the cationic substitution alters the critical equilibrium of the superexchange paths that make the magnetic structure stable and this fact might explain the appearance of new noncollinear magnetic structures.^{10,11}

M-type barium ferrite $\text{BaFe}_{12}\text{O}_{19}$ is being largely studied because of its high technological interest as a material suitable for perpendicular magnetic recording.¹² Many efforts have been devoted both to the development of a synthesis method that allows us to obtain fine particles,¹³⁻¹⁶ and to reduce its high intrinsic magnetocrystalline anisotropy.^{2,3} In this sense, several methods have been attempted to obtain suitable homogeneous, small-size particles and, on the other hand, *Ba-M* is usually doped with Co^{2+} ions,^{2,3,15,17-19} which are known to give a strong planar contribution to the anisotropy when located in octahedral

TABLE I. Crystallographic and magnetic characteristics of the metallic sublattices in the M -type $\text{BaFe}_{12-x}\text{Co}_x\text{Ti}_x\text{O}_{19}$ hexagonal ferrite.

Cation	Sublattice	Coordination	Block	No. ions per FU	Spin direction
$M1$	$2a$	octahedral	S	1	up
$M2$	$4e(\frac{1}{2})$	pseudotetrahedral	R	1	up
$M3$	$4f_{IV}$	tetrahedral	S	2	down
$M4$	$4f_{VI}$	octahedral	R	2	down
$M5$	$12k$	octahedral	R - S	6	up

sites,²⁰⁻²³ as it had been previously shown in cobalt-substituted magnetite.²⁴

We report in this work a study of the intrinsic structural and magnetic properties of the classical $\text{BaFe}_{12-2x}\text{Co}_x\text{Ti}_x\text{O}_{19}$ ($0 < x < 1$) doping scheme. The synthesis of all the polycrystalline samples used in this investigation was performed by the classical ceramic method² in order to avoid such problems as impurity formation¹⁷ and fine-particle effects.²⁵

Neutron powder diffraction has been proved an excellent technique to determine the cationic distribution in doped ferrites. In our present case, the scattering lengths of doping cations are smaller than that of Fe [$b(\text{Fe}) = 0.954$, $b(\text{Co}) = 0.25$, $b(\text{Ti}) = -0.33$, all in 10^{-12} cm] and then the average scattering length of each metallic site decreases when doping. For each sublattice where substitution takes place, we can write

$$b_i = y_i[b(\text{Co})] + z_i[b(\text{Ti})] + (1 - y_i - z_i)[b(\text{Fe})], \quad (1)$$

where the subscript i indicates the different sites, b_i are the average scattering lengths, and y_i and z_i represent, respectively, the population of Co and Ti ions substituted in a given i site. We will refer to them as the population parameters. In order to determine the values of y_i and z_i , we refine the average scattering length b_i of each metallic position, and the decrease of these b_i values is indicative of the substitution. On the other hand, if m_i represents the crystallographic multiplicity of a given i site per formula unit (FU), then $m_i y_i$ and $m_i z_i$ represent, respectively, the amount of Co and Ti ions substituted in this site per FU, in such a form that $\sum_i m_i y_i$ and $\sum_i m_i z_i$ are the total amounts of doping cations (Co and Ti, respectively) that have entered the structure per FU. When this total amount equals the nominal doping rate x , we have an additional equation, and thus we can construct a system of six equations with ten variables. Therefore, some physical hypotheses will be in order. We will show that the neutron-diffraction patterns allow the cation occupancy in each sublattice to be confined between two limits. Finally, the most plausible distribution at low doping levels is established from the measurement of the saturation magnetization.

II. EXPERIMENT

The synthesis of polycrystalline $\text{BaFe}_{12-2x}\text{Co}_x\text{Ti}_x\text{O}_{19}$ samples ($x = 0.2, 0.5, 0.7, 1.0$) was performed by high-temperature solid-state reactions of stoichiometric BaCO_3 , Fe_2O_3 , TiO_2 , and Co_3O_4 mixtures. Different firing temper-

atures between 1273 and 1473 K were chosen in order to optimize the reaction kinetics. Finally, all the compounds were fired at 1473 K for a period of several days with intermediate grindings and were quenched in air. The phase unicity of final samples was verified from both x-ray and neutron diffraction. We have restricted the nominal doping rate x to the interval $0 < x < 1.0$ since (i) the Curie temperature is still above the room temperature,^{2,15} (ii) the coercive field diminishes to technologically achievable values,^{2,15} and (iii) the overall magnetic structure remains ferrimagnetic.²⁶ Consequently, $\text{BaFe}_{12-2x}\text{Co}_x\text{Ti}_x\text{O}_{19}$ ($0 < x < 1.0$) M -type barium ferrites are suitable for magnetic perpendicular recording.

Neutron-powder-diffraction patterns were recorded at the D2B high-resolution diffractometer of the Institut Laue-Langevin with $\lambda = 1.594$ Å. This diffractometer is equipped with a bank of 64 detectors separated 2.5° in 2θ , each one equipped with Soller slits, allowing one to span an angular range of $2\theta = 160^\circ$; scanning the detector by 2.5° , in steps of 0.5° , one gets a full diffraction pattern. Several scan blocks are added to get better statistics and a good average for the detector positions. All the spectra were obtained both at $T = 793$ K in the paramagnetic phase and at $T = 4.2$ K in the ferrimagnetic phase and were analyzed with the Rietveld method of the STRAP software package.²⁷

The isothermal magnetization curves were measured at $T = 4.2$ K in a magnetic field up to $H = 200$ kOe by using a uniaxial extraction technique with a water-cooled Bitter magnet of the Service National des Champs Intenses in Grenoble.

III. EXPERIMENTAL RESULTS

A. Neutron powder diffraction

1. Paramagnetic phase ($T = 793$ K)

The cell and positional parameters together with the average scattering lengths b_i corresponding to the five metallic sublattices of the M structure and an isotropic temperature factor for each chemical species were simultaneously refined assuming the $P6_3/mmc$ space group. In Fig. 1(a) we show both the experimental and refined patterns for $x = 0.2$. The reduced chi-squared values were, in any case, below 5%, while the Bragg R factors were about 3%. No impurities were detected up to $x = 1.0$, thus any residual phase, if present in our Co-Ti-doping scheme, is below 1% in weight. From the refinement of the average scattering lengths b_i (Fig. 2), as defined in Eq. (1), it is evident that, although there is a partial substitution of Fe^{3+} ions by Co^{2+} - Ti^{4+} in all five metallic sublattices, the $2a$ octahedral and $4e(\frac{1}{2})$ pseudotetrahedral sites are much less sensitive to the doping rate than the other three sites (tetrahedral $4f_{IV}$, and octahedral $4f_{VI}$ and $12k$). The refined experimental error of all these b_i values was well below 2%. A complete analysis of both atomic distances and bonding angles, and their comparison to the Co-Sn-doping scheme, will be published soon elsewhere.

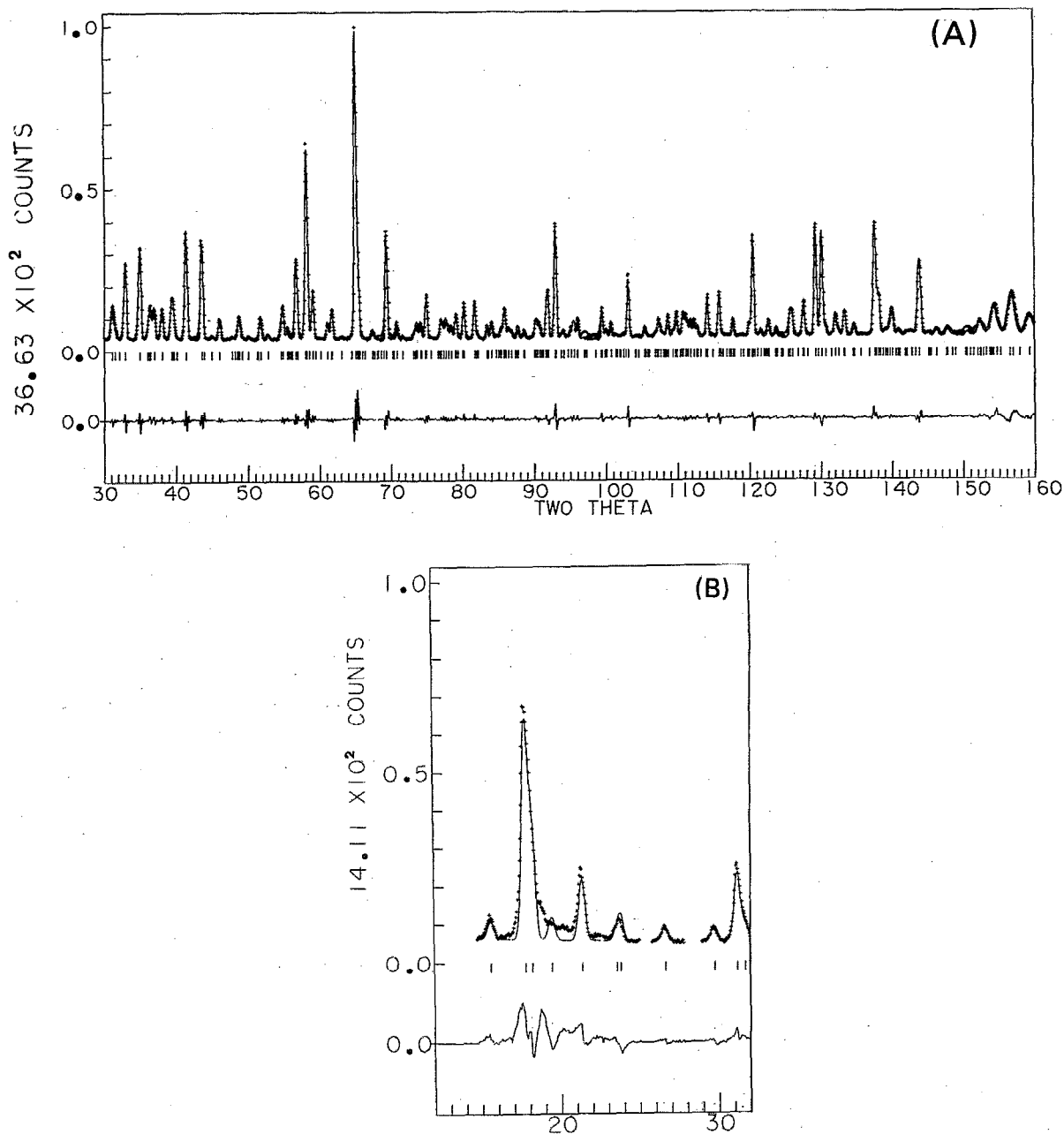


FIG. 1. Experimental and refined neutron-powder-diffraction patterns of $\text{BaFe}_{12-2x}\text{Co}_x\text{Ti}_x\text{O}_{19}$ compounds for (a) $x = 0.2$ at $T = 793$ K, and (b) $x = 1.0$ at $T = 4.2$ K (low-angle region).

2. Ferrimagnetic phase ($T = 4.2$ K)

We assume that (i) the average scattering lengths of the metallic sites do not change with respect to those refined in the paramagnetic phase, (ii) the magnetic form factor is that of Fe, since the total amount of Co^{2+} ions in the structure is small as compared to the amount of Fe^{3+} ions, and (iii) the magnetic structure can be described by the Gorter's model: uniaxial collinear structure, with three spin-up [$2a$, $4e(\frac{1}{2})$, and $12k$] and two spin-down ($4f_{\text{IV}}$ and $4f_{\text{VI}}$) sublattices.

The cell and positional parameters together with the magnetic moments of metallic sublattices and one isotropic temperature factor for each chemical element were simul-

taneously refined. The fitted magnetic moments of all metallic sublattices are represented in Fig. 3 as a function of the doping rate. The strong correlation existing among the magnetic moments of different sites is noticeable; for instance, we are not able to independently fit those corresponding to the $2a$ and $4e(\frac{1}{2})$ sites when $x = 1.0$. From these fitted values, we can easily derive the total magnetization per FU as

$$M_s^z = M(2a) + M(4e) - 2[M(4f_{\text{IV}})] - 2[M(4f_{\text{VI}})] + 6[M(12k)], \quad (2)$$

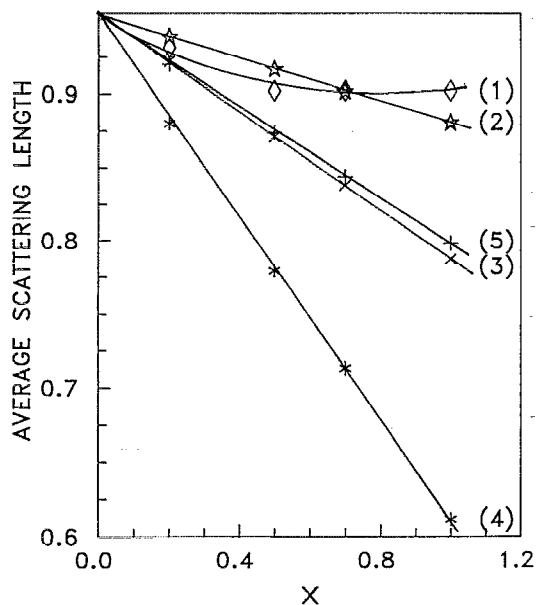


FIG. 2. Refined average scattering lengths b_i corresponding to the five metallic sublattices: (1) $2a$, (2) $4e(\frac{1}{2})$, (3) $4f_{IV}$, (4) $4f_{VI}$, and (5) $12k$, as a function of the doping rate x . For $x=0$, $b_i = b(\text{Fe}) = 0.954 \times 10^{-12}$ cm. All the represented values are given in 10^{-12} cm.

where M_s^n is given in μ_B/FU . (In Fig. 5 we show the compositional dependence of M_s^n .)

Concerning the goodness of the fit, the reduced chi-squared values are about 10% for all samples, while the Bragg nuclear and magnetic R factors are, respectively, about 6% and 7%, except for the Bragg magnetic R factor when $x=1.0$, which suddenly increases to 18%. If we carefully look at the low-angle region of the patterns, we observe that there exist both an extreme broadening of some Bragg peaks and a diffuse scattering [Fig. 1(b)], which are evident at doping rates higher than $x \approx 0.7$. These features are not caused by a residual percentage of impurities since no contribution of this kind appears in the paramagnetic patterns, thus showing their magnetic origin. This magnetic scattering might indicate that the strict collinearity of the magnetic structure is progressively broken when doping and that probably above $x \approx 0.7$ the magnetic ground state is no longer a collinear ferrimagnet but a disordered ferrimagnet which may be viewed as a precursor of the block-canted helimagnetic structure observed at higher x values ($x > 1.2$).²⁶

B. Isothermal magnetization measurements

Intrinsic magnetic parameters were obtained from a detailed analysis of isothermal $M(H)$ curves (Fig. 4). The law to approach to saturation (LAS) for ferromagnetic and ferrimagnetic powders can be written²⁸

$$M(H) = M_S(1 - A/H - B/H^2 - C/H^3) + \chi_d H, \quad (3)$$

where M_S is the saturation magnetization and χ_d the high-field differential susceptibility.

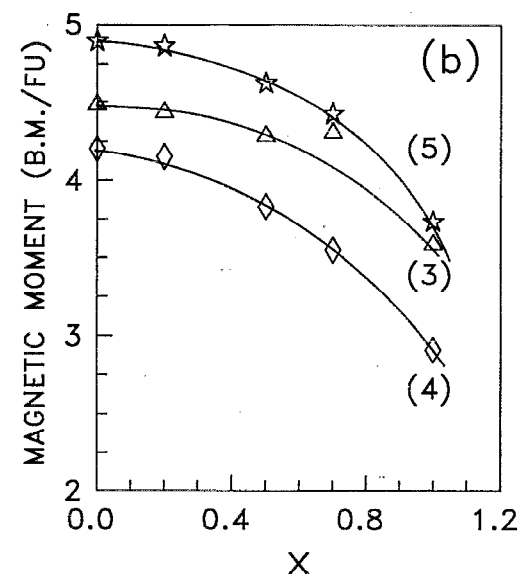
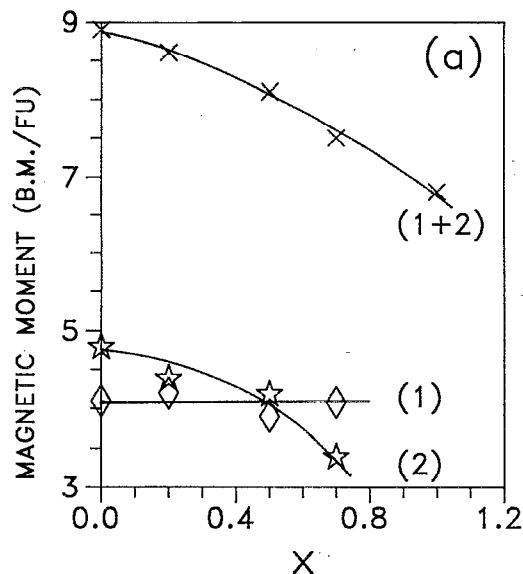


FIG. 3. Refined magnetic moments of the metallic sublattices. (a): (1) $2a$, (2) $4e(\frac{1}{2})$, and (1+2) $2a + 4e(\frac{1}{2})$; (b): (3) $4f_{IV}$, (4) $4f_{VI}$, and (5) $12k$. The $x=0$ values are given by Collomb and co-workers (Ref. 39).

The term A/H is attributed to the existence of inhomogeneities in the microcrystals which reduce the mobility of the magnetization²⁹ and from the theoretical point of view,³⁰ as has been experimentally found,³¹ it must vanish at high enough magnetic fields, otherwise the magnetic energy necessary to saturate the sample would be infinite. The second and the third terms are related to the magnetic anisotropy and can be written, for a uniaxial hexagonal compound with $K_2 \ll K_1$,³² as

$$\frac{B}{H^2} + \frac{C}{H^3} = \left(\frac{1}{15}\right) \left(\frac{H_a}{H}\right)^2 + \left(\frac{2}{105}\right) \left(\frac{H_a}{H}\right)^3,$$

$$H_a = 2K_1/M_S, \quad (4)$$

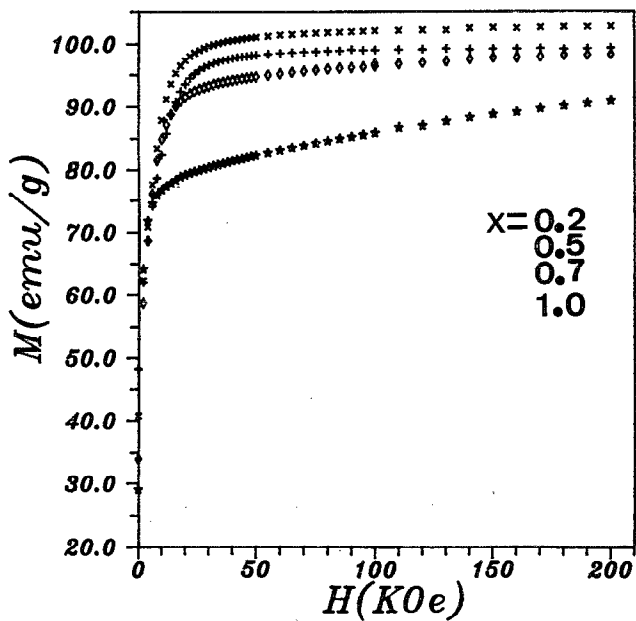


FIG. 4. Experimental isothermal magnetization curves $M(H)$ of the Co-Ti compounds, as a function of doping rate ($T = 4.2$ K).

where H_a is the anisotropy field, and K_1 and K_2 are the first and second anisotropy constants describing the magnetic anisotropy energy:²

$$E_a = K_1 \sin^2 \vartheta + K_2 \sin^4 \vartheta, \quad (5)$$

ϑ being the angle between the M vector and the hexagonal c axis.

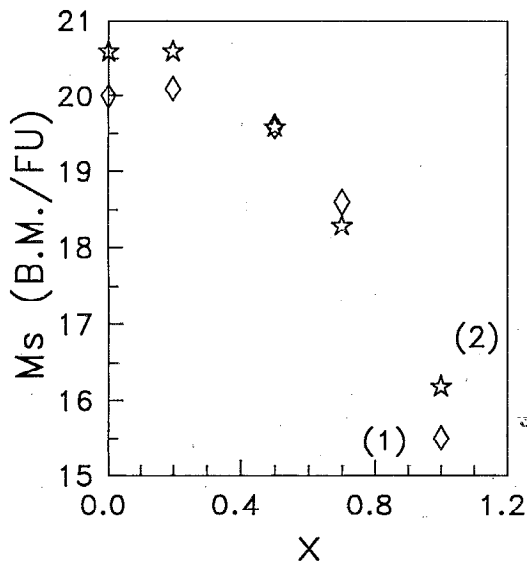


FIG. 5. Compositional dependence of the total magnetic moment per FU ($T = 4.2$ K), obtained from (1) isothermal magnetization curves (saturation magnetization) and (2) neutron powder diffraction [Eq. (2)]. For $x = 0$, see Refs. 11 and 39.

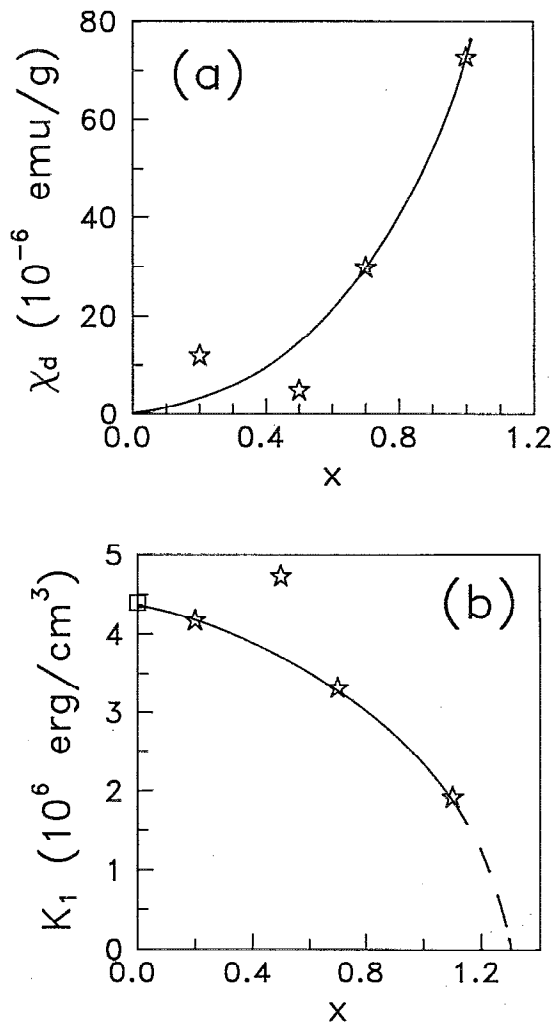


FIG. 6. Compositional dependence ($T = 4.2$ K) of (a) the high-field differential susceptibility χ_d and (b) the first anisotropy constant K_1 (the $x = 0$ value is given in Ref. 2).

Finally, the last term in Eq. (3) denotes the possibility of the existence of differential magnetic susceptibility,²⁸ which may appear when the magnetic structure becomes noncollinear.

Experimental $M(H)$ curves (Fig. 4) were fitted to Eq. (3) assuming that at high enough fields $A \approx 0$. In Fig. 5 we represent the compositional dependence of the experimental saturation magnetization M_S together with that obtained from the refinement of neutron-powder-diffraction patterns at $T = 4.2$ K [see Eq. (2)], M_S^n . In Fig. 6 we show the fitted values of the high-field susceptibility χ_d and the first anisotropy constant K_1 , obtained through Eqs. (3) and (4) assuming $K_2 \ll K_1$.

It is remarkable that above $x \approx 0.5$ there appear both a change in the decreasing slope of the experimental saturation magnetization and a sudden increase of the high-field susceptibility, thus indicating a strong increase of the noncollinearity in the magnetic structure. Although we are able to fit the overall magnetic structure to the collinear uniaxial model, the extreme broadening of some magnetic

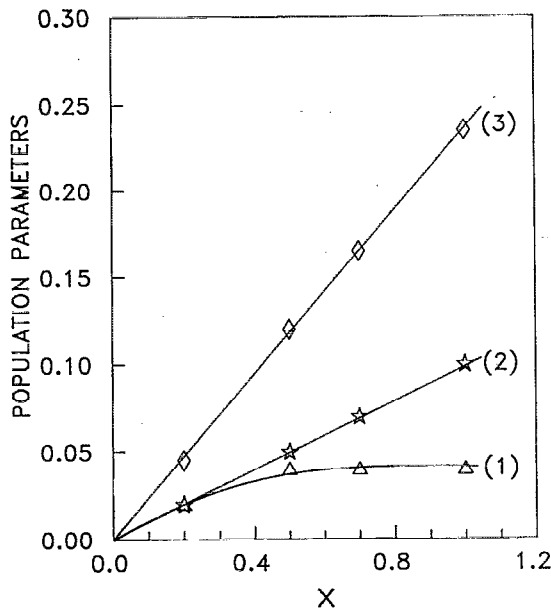


FIG. 7. Population parameters (1) z_1 (Ti^{4+} located in the octahedral $2a$ site), (2) y_2 [Co^{2+} located in the pseudotetrahedral $4e(\frac{1}{2})$], and (3) y_3 (Co^{2+} located in tetrahedral $4f_{IV}$ sites), as a function of the doping rate.

Bragg peaks observed in the low-angle region might indicate a short-range correlation among the magnetic noncollinear regions above $x \approx 0.7$, without this correlation leading to a true noncollinear long-range order. This interpretation would be in good agreement with the magnetic phase diagram proposed by Sadykov and co-workers.²⁶ Although the overall magnetic structure remains ferromagnetic up to $x \approx 1.2$, there exists a strong local spin canting, which may start to correlate at x values around $x \approx 0.7$, which finally could lead to a long-range helimagnetic structure above $x \approx 1.2$. On the other hand, we also note that our K_1 values deduced from the LAS on polycrystalline samples are also in good agreement with the reported values obtained from single-crystal studies: Our data indicate that the extrapolated value of K_1 becomes zero when $x \approx 1.3$, while Sadykov and co-workers²⁶ report that this occurs when $x = 1.4$. Anyway, our K_1 values are only indicative, since the method we have used to derive them does not allow us to evaluate higher-order terms, which are due to become important as the doping rate increases.^{3,20}

IV. ANALYSIS OF THE DATA AND DISCUSSION

Let us label, respectively, the $2a$, $4e(\frac{1}{2})$, $4f_{IV}$, $4f_{VI}$, and $12k$ as the 1, 2, 3, 4, and 5 sublattices. In order to solve the five equation system (1), some physical hypotheses are in order.

(i) We assume that Ti^{4+} ions do not enter tetrahedral sublattices ($z_2 = z_3 = 0$), which seems quite a plausible hypothesis within the low x values studied in this work, since it is experimentally well known that this cation has a marked preference for the octahedral sites.³³ In this sense, both the tetrahedral $4f_{IV}$ site and pseudotetrahedral

$4e(\frac{1}{2})$ sublattices are fully occupied by $\text{Fe}^{3+} + \text{Co}^{2+}$ ions and Eq. (1) allows us to unambiguously derive the population of Co^{2+} located in these two sites (Fig. 7). In this way, we obtain that the population of Co^{2+} ions substituted in the $4f_{IV}$ tetrahedral sites (y_3) follows, as a function of the doping rate x , the linear law

$$y_3 = 0.236(2)x,$$

$$m_3 y_3 = 0.47(1)x, \quad (6)$$

thus meaning that about 50% of the total amount of Co^{2+} that enters the structure does locate in these sites, which is in good agreement with those results reported by Kalvoda *et al.*⁴⁰ in the $\text{BaFe}_8\text{Co}_2\text{Ti}_2\text{O}_{19}$ M -type barium ferrite ($x = 2.0$), where $m_3 y_3 \approx 0.5x$.

(ii) Concerning the $2a$ octahedral site, the value of the substitution in this sublattice is much lower than in the other four and seems to saturate even at low doping rates. We have assumed in this work that no Co^{2+} enters this position ($y_1 = 0$), since this is actually the case at higher doping rates,⁴¹ so that from Eq. (1) we find that the population parameter z_1 of Ti^{4+} ions substituted in the $2a$ site (Fig. 7) varies from 0.018 when $x = 0.2$ to 0.04 when $x = 1.0$. Anyway, the substitution rates are so low that the global cationic distribution is not greatly affected by this choice; for example, if we assume that no Ti^{4+} enters this position ($z_1 = 0$), we derive that the population parameter y_1 of Co^{2+} ions substituted in this site varies from 0.016 when $x = 0.2$ to 0.07 when $x = 1.0$.

(iii) Finally, in order to determine the cationic distribution in the octahedral $4f_{VI}$ and $12k$ sublattices we assume that the total amount of Co^{2+} and Ti^{4+} that enters the structure is the same, although we do not restrict this value to the nominal doping rate x . This hypothesis provides us with a new equation:

$$m_2 y_2 + m_3 y_3 + m_4 y_4 + m_5 y_5 = m_1 z_1 + m_4 z_4 + m_5 z_5, \quad (7)$$

where $m_1 = 1$, $m_2 = 1$, $m_3 = 2$, $m_4 = 2$, and $m_5 = 6$ are the multiplicities of the different metallic sublattices per FU. We have reduced our original equation system to one of three equations [Eq. (1) written for $4f_{VI}$ and $12k$ sites plus Eq. (7)] having four variables. Giving values to z_4 and accepting as correct those solutions where the four unknowns are positive and monotonically increasing with the doping rate, we are able to restrict all the possible occupancies between two limiting cases, which we will call A and B limits, respectively. We can parametrize these two limiting cases by means of the ratio of the population parameters of the Co ions in the $12k$ and $4f_{VI}$ sublattices (and, consequently, by the same ratio of Ti ions), and we derive

	$y_5/y_4(\text{Co})$	$z_5/z_4(\text{Ti})$	
A Limit	∞	≈ 0.26 ,	
B Limit	0	≈ 1.33 .	(8)

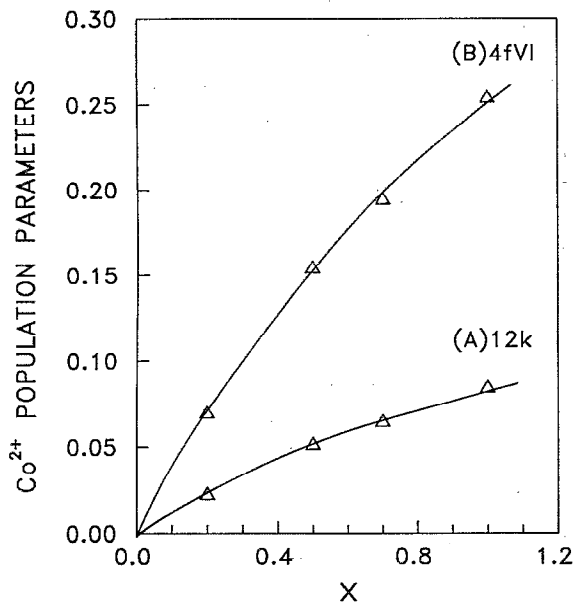


FIG. 8. Population parameters referred to Co^{2+} substituted in octahedral sites: (a) y_5 : $12k$ in the A limit (no Co ions located in the $4f_{\text{VI}}$ sublattice) and (b) y_4 : $4f_{\text{VI}}$ in the B limit (no Co ions located in the $12k$ sublattice).

In the A limit ($y_5/y_4 = \infty \Rightarrow z_5/z_4 \approx 0.26$), no Co^{2+} ions locate in the $4f_{\text{VI}}$ sublattice, while in the B limit ($y_5/y_4 = 0 \Rightarrow z_5/z_4 \approx 1.33$) no Co^{2+} are substituted in the $12k$ sublattice.

Any given cationic distribution having this ratio within these limiting cases is allowed. In order to clarify the hierarchy of preferences, we may look at the compositional dependence of the population parameters y_i and z_i . In Fig.

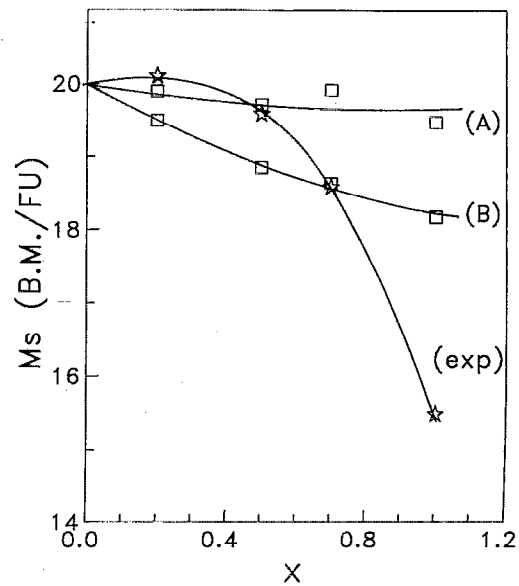


FIG. 10. Compositional dependence of the total magnetic moment per FU ($T = 4.2$ K) obtained from the cationic distribution in (a) the A limit, (b) the B limit, and (exp) experimental values (saturation magnetization).

8 the population of Co ions located in the $4f_{\text{VI}}$ (y_4) and $12k$ (y_5) sublattices in both limiting cases is displayed, while in Fig. 9 the same magnitudes are represented for Ti ions. We clearly observe that Ti ions basically show a hierarchy of preferences $4f_{\text{VI}} > 12k > 2a$ (Figs. 7 and 9), while for Co ions the hierarchy depends on the limiting case we choose (Figs. 7 and 8).

After all this procedure we find that the estimated relative error of the total amount of doping [evaluated from Eq. (7)] varies from 15% when $x = 0.2$ to 5% when $x = 1.0$. The nominal values are well within the estimated range.

In Fig. 10 we compare the experimental values of M_S with those obtained from the cationic distribution in the two limiting cases, assuming that the magnetic structure remains collinear. We assume $\mu(\text{Fe}) = 5 \mu_B$ and $\mu(\text{Ti}) = 0$. Concerning the magnetic moment of Co^{2+} ions, we assume the $3\text{-}\mu_B$ spin-only high-spin value when located in tetrahedral sites, and the $3.7 \mu_B$ value when located in octahedral sites.^{3,21,42} This latter is slightly higher than the spin-only high-spin value due to the partial quenching of the angular magnetic moment of these cations when located in octahedral sites.^{21,24} It is noticeable that the total magnetization derived from the A limit closely follows the experimental values up to $x \approx 0.5$, which means that, up to this doping rate, no Co^{2+} ions locate in the octahedral $4f_{\text{VI}}$ site (as has also been found both at higher doping rates⁴¹ and in the W -type $\text{BaCo}_2\text{Fe}_{16}\text{O}_{27}$ compound³⁹) and, consequently, a larger amount of Ti^{4+} ions occupy this sublattice in comparison to the $12k$ one. Figures 8 and 9 show that the cationic substitution in the $4f_{\text{VI}}$ and $12k$ sublattices in the A limit may be written, up to $x \approx 0.5$, as the following linear laws:

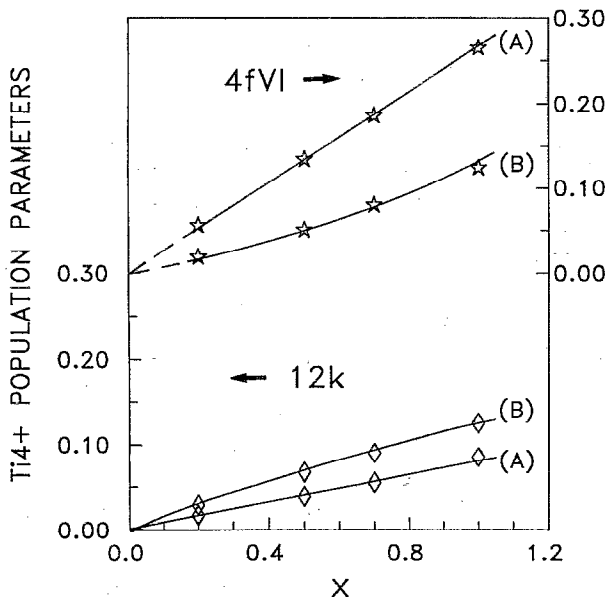


FIG. 9. Population parameters referred to Ti^{4+} substituted in octahedral $4f_{\text{VI}}$ (z_4) and $12k$ (z_5) sites in (a) the A limit ($z_5/z_4 \approx 0.26$) and (b) the B limit ($z_5/z_4 \approx 1.33$).

$$\begin{aligned}
y_4=0 &\Rightarrow \text{Co}(4f_{\text{VI}}): m_4 y_4=0, \\
y_5=0.103(6)x &\Rightarrow \text{Co}(12k): m_5 y_5=0.62(4)x, \\
z_4=0.27(1)x &\Rightarrow \text{Ti}(4f_{\text{VI}}): m_4 z_4=0.54(2)x, \\
z_5=0.078(3)x &\Rightarrow \text{Ti}(12k): m_5 z_5=0.47(2)x. \quad (9)
\end{aligned}$$

We believe that this is a fairly realistic evaluation of the cationic distribution in this compositional range, although it is obvious that this hierarchy of preferences may be strongly modified at higher substitution rates because of the perturbed charge distribution among the different sublattices. A further support to our assumption of a collinear magnetic structure up to $x \approx 0.5$ comes from the fact that the strong increase of the high-field susceptibility takes place at $x > 0.5$. Consequently, the magnetic structure seems to remain collinear up to this doping rate thus validating our choice of the cationic distribution corresponding to the A limit from the spontaneous magnetization measurements.

At higher doping values, the increase of the high-field magnetic susceptibility indicates that some degree of local spin canting appears. Then, no conclusion may be drawn from the experimental magnetization values concerning the cation distribution. Finally, above $x \approx 0.7$ the differences between experimental and deduced data indicate a strong increase of the magnetic noncollinearity.

V. SUMMARY AND CONCLUSIONS

Our neutron-powder-diffraction study of the Co-Ti series in the paramagnetic phase has allowed us to ascertain that the $2a$ octahedral and $4e(\frac{1}{2})$ pseudotetrahedral sublattices are nearly fully occupied with Fe^{3+} ions (less than 10% of substitution), while, within the explored substitution rate, a considerable amount of Co^{2+} (about 50% of the nominal doping rate) occupy the tetrahedral site $4f_{\text{IV}}$, thus being ineffective, according to the single-ion theory of anisotropy, in the reduction of the magnetic anisotropy.³⁴ These results are agreement with those reported by Collomb and co-workers³⁵ in the Y-type $\text{Ba}_2\text{Co}_2\text{Fe}_{11}\text{O}_{22}$ compound, in which a considerable amount of Co^{2+} ions located in tetrahedral sites. In our samples, we observe that the total amount of Co ions located in tetrahedra [tetrahedral $4f_{\text{IV}}$ plus pseudotetrahedral $4e(\frac{1}{2})$ sublattices] is about 10% greater than the total amount located in octahedra, which implies a marked preference of Co^{2+} ions for the tetrahedral sites (Fig. 11). At the same time, in the framework of the Stoner-Wohlfarth model, the lowering of the coercive field in single-domain particles signals that the anisotropy decreases.³⁶ In a previous work we reported that a larger quantity of Co locates in tetrahedra when doping with Co-Ti than when doping with Co-Sn,¹⁷ thus matching the fact that in the latter the coercive field decreases with the doping rate faster than in the former.^{2,15,18,37} This fact emphasizes the importance of the nonmagnetic counter ions on doping M-type Ba ferrite with Co^{2+} . Referring to the octahedral $4f_{\text{VI}}$ and $12k$ sublattices we have restricted from neutron-diffraction measurements the possible occupancies within two limiting

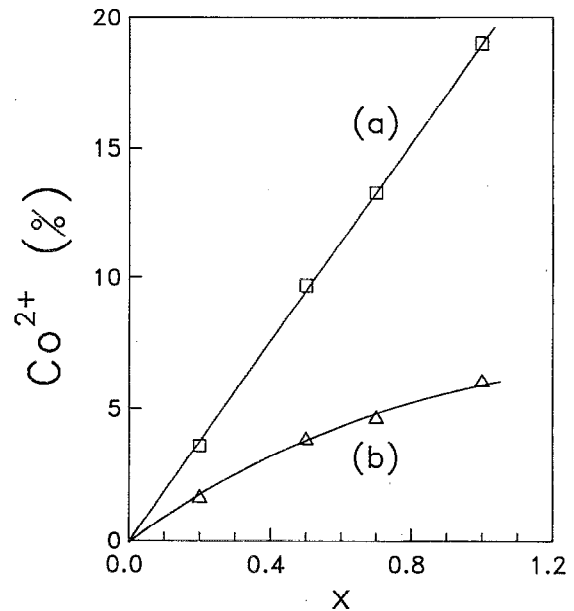


FIG. 11. Percentage of Co^{2+} ions located in (a) tetrahedral and (b) octahedral sites.

cases: in the A limit ($y_5/y_4 = \infty \Rightarrow z_5/z_4 \approx 0.26$), no Co^{2+} ions locate in the $4f_{\text{VI}}$ sublattice, while in the B limit ($y_5/y_4 = 0 \Rightarrow z_5/z_4 \approx 1.33$) no Co^{2+} are substituted in the $12k$ sublattice.

Magnetization measurements and neutron-powder-diffraction patterns at low temperature allow us to decide which of the two limiting cases stands for the real cationic distribution, and to develop a primary framework of how the magnetic structure and the intrinsic magnetic parameters are modified when doping. Concerning the cationic distribution it seems clear that, up to $x \approx 0.5$, no Co^{2+} ions locate in the $4f_{\text{VI}}$ site and, consequently, Ti^{4+} ions prefer this site to the $12k$ one (A limit). In this compositional range ($x < 0.5$), the most plausible amount of doping cations per FU in the different metallic sublattices may thus be expressed by means of the following linear laws:

$$\begin{aligned}
\text{Co}(2a): \quad m_1 y_1 &= 0, \\
\text{Co}[4e(\frac{1}{2})]: \quad m_2 y_2 &= 0.10(1)x, \\
\text{Co}(4f_{\text{IV}}): \quad m_3 y_3 &= 0.47(1)x, \\
\text{Co}(4f_{\text{VI}}): \quad m_4 y_4 &= 0, \\
\text{Co}(12k): \quad m_5 y_5 &= 0.62(4)x, \\
\text{Ti}(2a): \quad m_1 z_1 &= 0.08(1)x, \\
\text{Ti}[4e(\frac{1}{2})]: \quad m_2 z_2 &= 0, \\
\text{Ti}(4f_{\text{IV}}): \quad m_3 z_3 &= 0, \\
\text{Ti}(4f_{\text{VI}}): \quad m_4 z_4 &= 0.54(2)x, \\
\text{Ti}(12k): \quad m_5 z_5 &= 0.47(2)x. \quad (10)
\end{aligned}$$

Concerning the considerable amount of Co^{2+} ions located in tetrahedral sites either in the M-type structure⁴⁰ or in the Y-type structure,³⁵ these results (and our own re-

sults reported in the present study) differ from the conventional school of thought on the site occupancy of Co^{2+} ions. In the past, several authors pointed out, from the dependence of the saturation magnetization on the doping rate or from the microwave ferromagnetic resonance,²² the strict preference of Co^{2+} ions for the octahedral sites. We believe that this assertion could be uncertain due to the large number of possible cationic distributions among the metallic sublattices of these hexagonal structures. In this sense, neutron diffraction is a more accurate technique to determine the cationic distribution.

Above $x \approx 0.5$, the noncollinear spin structure does not allow us to decide whether this tendency changes or not. On the other hand both the strong decrease of the experimental saturation magnetization and the sudden increase of the high-field differential susceptibility above $x \approx 0.7$ suggest that the collinearity of the magnetic structure is lost above this doping concentration. These results match both the anomalies observed in the low-angle region of the low-temperature diffraction patterns and the differences between the experimental magnetization values and those derived from the cationic distribution assuming uniaxial collinear magnetic structure. All these facts strongly suggest that the disorder associated to the cation substitution introduces some kind of local spin canting as a consequence of the suppression of some superexchange interactions.

Our results are in good agreement with those given by Sadykov and co-workers²⁶ in monocrystalline samples: Although the overall magnetic structure of the Co-Ti series seems to remain ferrimagnetic up to $x \approx 1.2$, there exists a strong local noncollinearity. In this sense, the low-angle diffuse magnetic scattering observed on neutron-diffraction patterns for $x > 0.7$ might indicate the development of some spatial correlation among the noncollinear spin components.

Our data do not allow a straightforward analysis of the origin of the breakdown of the spin collinearity, although it might be speculated that the preferential occupancy, by nonmagnetic Ti^{4+} ions, of the $4f_{\text{VI}}$ sites, gives rise to the weakening of the strong $12k-4f_{\text{VI}}$ superexchange path and thus approaches the isotropic exchange energy to other second-order terms on the magnetic Hamiltonian, such as the antisymmetric interaction³⁸ or even the magnetocrystalline anisotropy. The octahedral $12k$ site is found to be very sensitive to nonmagnetic substitution in the nearest-neighbor sites ($4f_{\text{VI}}$ and $4f_{\text{IV}}$) as a result of the fact that it is the one where the competing interactions are stronger and, consequently, the stabilization energy is the lowest among all five metallic sublattices.⁸

Last but not least, it is straightforward to note that, concerning the applicability of Co^{2+} -doped M -type Ba ferrite as perpendicular recording media, a considerable improvement of the cobalt octahedral occupancy rate should be obtained in order to get a faster reduction of the magnetocrystalline anisotropy with the doping rate. In this way, the degree of substitution required on the basis of coercivity of single-domain particles could be reduced and thus the saturation magnetization would become less per-

turbed. As it has been mentioned, considerable differences in the Co tetrahedral-site occupancy are observed with other counterions, such as Sn^{4+} .^{17,18,37} It appears then that a wide investigation on the effect of the different counterions on the Co distribution would be worthwhile so as to improve the characteristics of the Ba ferrite small particles developed as perpendicular magnetic and Ba ferrite thin films as magneto-optic recording media.¹

ACKNOWLEDGMENTS

We are grateful to the Service National des Champs Intenses and to the Institut Laue Langevin for allowing us to use their technical facilities. The financial support of the Ministerio de Educación y Ciencia, Spain, and of C.S.I.C.-C.N.R.S. through a Programme International de Coopération Scientifique (P.I.C.S.) project is also recognized.

- ¹M. P. Sharrock, IEEE Trans. Magn. MAG-25, 4374 (1989); M. H. Kryder, J. Magn. Mater. 83, 1 (1990); P. Gerard, E. Lacroix, G. Marest, M. Duphy, G. Rolland, and B. Blanchard, J. Magn. Mater. 83, 13 (1990).
- ²H. Kojima in *Ferromagnetic Materials*, edited by E. P. Wohlfarth (North-Holland, Amsterdam, 1982), Vol. 3.
- ³J. Smit and H. P. J. Wijn, *Ferrites* (Philips Technical Library, Eindhoven, 1960).
- ⁴X. Obradors, A. Collomb, M. Pernet, D. Samaras, and J. C. Joubert, J. Solid State Chem. 56, 171 (1985).
- ⁵E. W. Gorter, Proc. IEEE 104B, 225 (1957).
- ⁶G. Albanese, J. Phys. (Paris) Colloq. 38, C1-85 (1977).
- ⁷H. A. Kramers, Physica 1, 182 (1934); P. W. Anderson, Phys. Rev. 76, 350 (1950); 76, 705 (1950).
- ⁸A. Isalgué, A. Labarta, J. Tejada, and X. Obradors, Appl. Phys. A 38, 3063 (1985).
- ⁹G. Albanese, M. Carbuicchio, and A. Deriu, Phys. Status Solidi A 23, 351 (1974).
- ¹⁰G. Albanese, G. Asti, and P. Batti, Nuovo Cimento B 54, 339 (1968); 58, 467 (1968); 58, 480 (1968); O. P. Aleshko-Ozhevskii and I. I. Yamzin, Sov. Phys. JETP 29, 155 (1969); M. I. Namtalishvili, O. P. Aleshko-Ozhevskii, and I. I. Yamzin, Sov. Phys. Solid State 13, 2137 (1972); G. Albanese, A. Deriu, E. Carbuicchio, and G. Slokar, Appl. Phys. A 26, 45 (1981).
- ¹¹X. Obradors, A. Isalgué, A. Collomb, M. Pernet, J. Pannetier, J. Rodríguez, J. Tejada, and J. C. Joubert, IEEE Trans. Magn. MAG-20, 1636 (1984); X. Obradors, A. Collomb, M. Pernet, and J. C. Joubert, J. Magn. Mater. 44, 118 (1984); A. Collomb, X. Obradors, A. Isalgué, and D. Fruchart, J. Magn. Mater. 69, 317 (1987).
- ¹²S. Iwasaki, IEEE Trans. Magn. MAG-20, 654 (1984); M. Suzuki, *ibid.*, MAG-20, 675 (1984).
- ¹³W. Ross, J. Am. Ceram. Soc. 63, 601 (1980).
- ¹⁴M. Kiyara, T. Yakada, N. Nagai, and N. Horiishi, Adv. Ceram. 15, 51 (1985).
- ¹⁵O. Kubo, T. Ido, and H. Yokoyama, IEEE Trans. Magn. MAG-18, 1112 (1982); O. Kubo, T. Ido, H. Yokoyama, and Y. Koike, J. Appl. Phys. 57, 4280 (1985).
- ¹⁶F. Licci and T. Besagni, IEEE Trans. Magn. MAG-20, 1639 (1984); M. Vallet, P. Rodríguez, X. Obradors, A. Isalgué, J. Rodríguez, and M. Pernet, J. Phys. (Paris) Colloq. 46, C6-335 (1985).
- ¹⁷X. Batlle, J. Rodríguez, X. Obradors, M. Pernet, M. Vallet, and J. Fontcuberta, J. Phys. (Paris) Colloq. 49, C8-939 (1988).
- ¹⁸X. Batlle, M. Pernet, X. Obradors, and M. Vallet, in *Advances in Ferrites*, edited by C. M. Srivastava and M. J. Patni (Oxford and IBH, New Delhi, 1989).
- ¹⁹X. Batlle, X. Obradors, M. Pernet, M. Vallet, M. V. Cabañas, J. Rodríguez, and J. Fontcuberta, J. Magn. Mater. 83, 465 (1990).
- ²⁰F. Bolzoni and L. Pareti, J. Magn. Mater. 42, 44 (1984).
- ²¹F. Chou, X. Feng, J. Li, and Y. Lin, J. Appl. Phys. 61, 3381 (1987).
- ²²D. J. De Bitetto, J. Appl. Phys. 35, 3482 (1964).
- ²³F. Dionne, J. Appl. Phys. 64, 1323 (1988).
- ²⁴J. C. Slonczewski, Phys. Rev. 110, 1341 (1958).

- ²⁵ A. H. Morrish and K. Haneda, *J. Magn. Magn. Mater.* **35**, 105 (1983); O. Kubo, T. Ido, H. Yokoyama, and Y. Koike, *J. Appl. Phys.* **57**, 4280 (1985); S. Kiruso, T. Ido, and H. Yokoyama, *IEEE Trans. Magn. MAG-23*, 3137 (1987); K. Haneda, *Can. J. Phys.* **65**, 1233 (1987).
- ²⁶ R. A. Sadykov, O. P. Aleshko-Ozhevskii, and N. A. Arten'em, *Sov. Phys. Solid State* **23**, 1090 (1981); R. A. Sadykov (private communication).
- ²⁷ H. M. Rietveld, *Acta Cryst.* **22**, 151 (1967); *J. Appl. Cryst.* **2**, 65 (1969); J. Rodríguez, J. Pannetier, and M. Anne, STRAP, Institut Laue-Langevin Internal Report No. 87Ro14T, 1987.
- ²⁸ R. Grossinger, *Phys. Status Solidi A* **66**, 665 (1981); *J. Magn. Magn. Mater.* **28**, 137 (1982).
- ²⁹ L. Néel, *J. Phys. (Paris)* **9**, 148 (1948); *J. Phys. Radium* **9**, 184 (1948).
- ³⁰ L. Néel, *J. Phys. (Paris)* **9**, 193 (1948).
- ³¹ A. T. Aldred and P. H. Froehle, *Int. J. Magn.* **2**, 195 (1972).
- ³² N. Akulov, *Z. Phys.* **69**, 822 (1931); R. Graus, *Ann. Phys.* **15**, 28 (1932).
- ³³ N. C. Greenwood, *Cristales Iónicos, Defectos Reticulares y no Estequiometría* (Alambra, Madrid, 1970).
- ³⁴ A. Herpin *Théorie du Magnetisme* (P.U.F., Paris, 1967).
- ³⁵ A. Collomb, M. A. Hadj Farhat, and J. C. Joubert, *Mater. Res. Bull.* **24**, 459 (1989).
- ³⁶ E. C. Stoner and E. P. Wohlfarth, *Philos. Trans. R. Soc. (London) Ser. A* **240**, 599 (1948).
- ³⁷ M. Pernet, X. Obradors, M. Vallet, T. Hernandez, and P. Germi, *IEEE Trans. Magn. MAG-24*, 1998 (1988).
- ³⁸ I. Dzyaloshinsky, *J. Appl. Chem. Solids* **4**, 241 (1958); T. Moriya, *Phys. Rev.* **120**, 92 (1960).
- ³⁹ A. Collomb, P. Wolfers, and X. Obradors, *J. Magn. Magn. Mater.* **62**, 57 (1986).
- ⁴⁰ L. Kalvoda, M. Dlouhá, S. Vratislav, and Z. Jiráček, *J. Magn. Magn. Mater.* **87**, 243 (1990).
- ⁴¹ X. Batlle, M. V. Cabañas, X. Obradors, M. Vallet, and J. Rodríguez-Carvajal, in *Spanish Contribution to Neutron Scattering Techniques* (in press).
- ⁴² G. Alabanese, M. Carbucicchio, A. Deriu, G. Asti, and S. Rinaldi, *Appl. Phys.* **7**, 227 (1987).